Simplicial SIRS epidemic models with nonlinear incidence rates

Cite as: Chaos **31**, 053112 (2021); https://doi.org/10.1063/5.0040518
Submitted: 14 December 2020 . Accepted: 18 April 2021 . Published Online: 13 May 2021

Dong Wang, Yi Zhao, Jianfeng Luo, and Hui Leng

Simplicial SIRS epidemic models with nonlinear incidence rates

Cite as: Chaos **31**, 053112 (2021); doi: 10.1063/5.0040518
Submitted: 14 December 2020 · Accepted: 18 April 2021 ·
Published Online: 13 May 2021

Dong Wang, Yi Zhao,[a] Jianfeng Luo, and Hui Leng

AFFILIATIONS

School of Science, Harbin Institute of Technology (Shenzhen), Shenzhen 518055, China

[a]**Author to whom correspondence should be addressed:** zhao.yi@hit.edu.cn

ABSTRACT

Mathematical epidemiology that describes the complex dynamics on social networks has become increasingly popular. However, a few methods have tackled the problem of coupling network topology with complex incidence mechanisms. Here, we propose a simplicial susceptible-infected-recovered-susceptible (SIRS) model to investigate the epidemic spreading via combining the network higher-order structure with a nonlinear incidence rate. A network-based social system is reshaped to a simplicial complex, in which the spreading or infection occurs with nonlinear reinforcement characterized by the simplex dimensions. Compared with the previous simplicial susceptible-infected-susceptible (SIS) models, the proposed SIRS model can not only capture the discontinuous transition and the bistability of a complex system but also capture the periodic phenomenon of epidemic outbreaks. More significantly, the two thresholds associated with the bistable region and the critical value of the reinforcement factor are derived. We further analyze the stability of equilibrium points of the proposed model and obtain the condition of existence of the bistable states and limit cycles. This work expands the simplicial SIS models to SIRS models and sheds light on a novel perspective of combining the higher-order structure of complex systems with nonlinear incidence rates.

In recent years, the network-based mathematical models have played a vital role in understanding spreading dynamics. The structures of a complex network confined to nodes and links are widely used to characterize pairwise interactions between individuals, but they make the incidence rates mathematically bilinear so that many underlying dynamical phenomena cannot be captured at length. To address this issue, we adopt simplicial complexes to describe collective interactions, thereby building a higher-order simplicial SIRS epidemic model with a nonlinear incidence rate. In addition to the discontinuous transitions and bistable states that occur in simplicial SIS models, the proposed SIRS model further appears to be stable limit cycles. Our findings shed light on a new perspective for modeling higher-order spreading processes with consideration of nonlinear incidence rates and demonstrate the importance of higher-order structure for understanding the effect of collective interactions on complex systems.

I. INTRODUCTION

Mathematical models with applications to the complex network are widely used to understand many social phenomena, from epidemic spreading[1] to information diffusion[2,3] to opinion formation.[4,5] Taking the epidemic spreading in a complex network as an example, the typical assumption is that the transmission process that occurs is based on the pairwise interaction of node to node, in which the infectious node and the susceptible node are connected by a link. Many useful approaches are developed to describe spreading processes, such as the mean-field method,[6] Markov chain approach,[7] message passing approach,[8] effective degree approach,[9] and epidemic link equation method.[10] Moreover, great progress has been achieved in the network spreading dynamics, such as the discovery of the propagation threshold,[11,12] the interplay between information and epidemic in multiplex networks,[13,14] the localization of epidemics,[15,16] the containment of epidemics,[17,18] and the detection of vital spreaders.[19–21]

However, the previous network-based works do not consider collective interactions among the components of social systems, but the link-based pairwise interaction. In reality, besides the pairwise interaction between nodes, many viruses can also be transmitted through collective interactions, such as social gathering behaviors,[22] where aerosol[23,24] plays an important role. Despite the fact that pairwise interactions have been well developed to describe propagation dynamics on social systems, a few attempts have been made at

studying the collective interactions. The limitation of complex networks is that their structural elements (i.e., nodes and links) are suitable to describe pairwise interactions but appear to be inadequate to describe collective interactions.[25]

To relax the structural limitation of complex networks, it is necessary to introduce higher-order models of which simplicial complexes and hypergraphs are the two popular tools.[25–27] Bode *et al.* propose a SIS epidemic spreading defined on a hypergraph with a focus on the community structure and the nonlinear dependence of the infected neighbors.[28] More significantly, Iacopini *et al.* present a social contagion model on simplicial complexes by introducing a reinforcement mechanism of simplices of order two.[29] Based on hypergraphs, Arruda *et al.* investigate the social contagion and phase transitions,[30,31] and Carletti *et al.* study the random walk and apply it to node ranking and classification tasks.[32] Higham *et al.* study a SIS model on hypergraphs to analyze spectral thresholds for epidemic extinction.[33] Based on simplicial complexes, Torres *et al.* investigate the spectral properties of a simplicial complex and discuss the implications for higher-order diffusion.[34] Wang *et al.* study a coupling communication model of idea integration and information transmission.[35] Burgio *et al.* analyze the dynamical effects of group interactions on contagion processes.[36] The characterization of higher-order structures and dynamical processes on them has attracted more and more attention.

In the research of network spreading dynamics, the incidence rates are usually assumed to be bilinear, i.e., the incidence rate of a node is proportional to the susceptible probability of the node and the infectious probability of its neighbors, respectively.[37–39] However, the reality is not always such case for many infectious diseases,[40,41] especially for the system with rich collective interactions as the state of surrounding individuals can change the disease concentration.[42,43] Meanwhile, for an ordinary differential equation (ODE) epidemic model in biomathematics, nonlinear incidence rates are widely adopted to capture various dynamical features,[44–48] such as saddle-node bifurcation, stable limit cycles, and Hopf bifurcation. Note that there are different forms of nonlinear incidence rates in ODE epidemic models. Let $S(t)$ and $I(t)$ be the number of susceptible and infective individuals at time t, respectively. Capasso and Serio[44] propose a saturated incidence rate $g(I)S$ to study the cholera epidemic, where $g(I)$ decreases when I is large enough. Liu *et al.* propose an incidence rate, $\beta I^p S^q$,[45,46] to study the codimension-1 bifurcation for SIRS and SEIRS models. Nonlinear incidence rates in the forms of $kI^2S/(1+\alpha I^2)$[47] and $\beta SI(1+\nu I^q)$[40,48,49] are also considered in some epidemiological models. Inspired by the application of nonlinear incidence rates in ODE models, we introduce it to study the spreading dynamics on social systems with higher-order structures.

Most of the previous epidemic models that consider the topological structure of social systems usually focus on the simple SIS or SIR model. However, in many instances, the SIS or SIR model may be inadequate to describe a complicated spreading process, and, therefore, another typical compartment model, SIRS,[50] is proposed to capture complicated dynamical behaviors of epidemic spreading systems. In this paper, inspired by the work in Ref. 29, we expand the SIS model to a SIRS model based on simplicial complexes by coupling a nonlinear incidence rate and higher-order structures of complex networks. We perform numerical simulations on real-world and synthetic data to investigate the proposed model and then give the theoretical analysis based on the mean-field approach. Besides the discontinuous transition and bistable state that have occurred in the SIS model, numerical experiments and theoretical analysis demonstrate the periodic phenomena of epidemic outbreaks in the SIRS model. Moreover, distinct from the SIS model, we conduct a detailed stability analysis for the SIRS model and investigate how the critical initial values affect the stationary state in a bistable region.

The paper is organized as follows. In Sec. II, we expose the simplex-based SIRS model with consideration of nonlinear incidence. In Sec. III, we perform numerical simulations on empirical and synthetic simplicial complexes. In Sec. IV, theoretical analysis is conducted by using the mean-field method. We close this paper in Sec. V with conclusions.

II. SIMPLICIAL SIRS MODEL

In a comparison with complex networks composed of nodes and links, simplicial complexes are more suitable to characterize collective interactions because they can describe higher-order structures of a system. However, the structure of many kinds of systems is stored in the data form of complex networks.[26] In a sense, it is necessary to detect the underlying higher-order structure of a complex network to investigate the collective interactions of a system.[51,52] Note that a real complex network can be regarded as the projection of the high-dimension topological structure of complex systems. By constructing its simplicial complexes, the higher structures hidden in the complex network could be revealed.[25] The co-presence contact data or data in the form of such sets (like co-authorship data[53] used in this paper) already show the utility of simplicial complexes. But given a synthetic pairwise complex network, the high-order topology may not exist or is unknown. By promoting each clique of such a network to the simplex,[54] the simplicial complexes can be constructed,[55,56] which is an alternative approach to investigate the higher-order interactions limited by the pairwise fashion of complex network. We recall that a d-simplex σ_d is a set of $d+1$ nodes $\sigma_d = [n_0, n_1, \ldots, n_d]$, where d is the dimension of σ_d. Any subset $\sigma_{d'}(d' \leqslant d)$ of σ_d is its subsimplex, which is called "face" in algebraic topology.[57] Taking 2-simplices as an example, besides the three nodes $[n_0]$, $[n_1]$, and $[n_2]$ that represent individuals, it contains three links $[n_0, n_1]$, $[n_0, n_2]$, and $[n_1, n_2]$ that denote pairwise interactions and a "full" triangle $[n_0, n_1, n_2]$ for a higher-order interaction. The simplicial complex is the collection of all these simplices. For a system of N nodes, similar to the definition of the adjacency matrix of a complex network, we use an adjacency tensor[58] $\mathscr{A}_{d'} = \{a_{i_0,i_1,\ldots,i_{d'}}\}_{i_0,i_1,\ldots,i_{d'}=1}^{N}$ $(d' = 0, \ldots, d)$ to denote a uniform simplicial complex with all simplex dimensions d', where $a_{i_0,i_1,\ldots,i_{d'}} = 1$ if nodes $n_{i_0}, n_{i_1}, \ldots, n_{i_{d'}}$ form a d'-simplex and $a_{i_0,i_1,\ldots,i_{d'}} = 0$ otherwise. In particular, $\mathscr{A}_1 = \{a_{i,j}\}_{i,j=1}^{N}$ coincides with the adjacency matrix of complex networks, and $\mathscr{A}_2 = \{a_{i,j,k}\}_{i,j,k=1}^{N}$ characterizes two-dimensional simplices: $a_{i,j,k} = 1$, if the three nodes n_i, n_j, and n_k form a full triangle and $a_{i,j,k} = 0$, otherwise. Therefore, the connectivity structure of a simplicial complex is described by the entire set of $d+1$ adjacency tensors, i.e., $\mathscr{A} = \{\mathscr{A}_0, \mathscr{A}_1, \ldots, \mathscr{A}_d\}$. Note that the simplicial complex degenerates into the complex network when the largest dimension of its simplices is $d = 1$.

Next, we build a simplicial SIRS model with a nonlinear incidence rate. Here, we adopt the nonlinear incidence rate $\beta SI(1+\nu_{d'}I^{d'})$, a variant of $\beta SI(1+\nu I^{q})$,[40] to describe the dynamic characteristics of a higher-order model, where $\nu_{d'}$ $(\geqslant 0)$ denotes the enhancement effect of the collective interaction of a d' dimensional simplex and β is the infectivity parameter. We select this nonlinear incidence rate because it can associate well with the higher-order structures of simplicial complexes. Let $V=\{\nu_{d'}\}_{d'=1}^{d}$ denote the set of the enhancement factor for different dimensional simplices, where $\nu_2=\nu_\Delta$ corresponds to the enhancement effect of 2-simplices and $\nu_1=1$ for the pairwise interaction in this model. We employ the quenched mean-field method[59] to describe the simplicial SIRS compartment model in detail. The state probabilities of susceptible (S), infective (I), and recovery (R) of node n_i at time t are defined by $p_i^S(t)$, $p_i^I(t)$, and $p_i^R(t)$, respectively. The dynamical system is presented as below:

$$\begin{aligned}
\frac{dp_i^S(t)}{dt} &= -\beta p_i^S(t)\left[\sum_{j=1}^{N} a_{ij}p_j^I(t)+\sum_{d'=1}^{d}\nu_{d'}\sum_{j_0,\ldots,j_{d'-1}} a_{i,j_0j_1\cdots j_{d'-1}}\prod_{k=0}^{d'-1}p_{j_k}^I(t)\right]+\gamma p_i^R(t),\\
\frac{dp_i^I(t)}{dt} &= \beta p_i^S(t)\left[\sum_{j=1}^{N} a_{ij}p_j^I(t)+\sum_{d'=1}^{d}\nu_{d'}\sum_{j_0,\ldots,j_{d'-1}} a_{i,j_0j_1\cdots j_{d'-1}}\prod_{k=0}^{d'-1}p_{j_k}^I(t)\right]-\mu p_i^I(t),\\
\frac{dp_i^R(t)}{dt} &= \mu p_i^I(t)-\gamma p_i^R(t),
\end{aligned} \tag{1}$$

where β, μ, and γ denote the probabilities of infection, recovery, and losing immunity, respectively. $\beta p_i^S(t)\sum_j a_{ij}p_j^I(t)$ represents the pairwise interaction that a S-state node n_i can get the infection from an I-state neighbor n_j through link $[n_i,n_j]$ with the probability β (corresponding to the process $S+I\xrightarrow{\beta}2I$). The term $\beta p_i^S(t)\nu_{d'}\sum_{j_0,\ldots,j_{d'-1}}a_{i,j_0j_1\cdots j_{d'-1}}\prod_{k=0}^{d'-1}p_{j_k}^I(t)$ is introduced to represent the collective interaction that a S-state node n_i can be infected by its d' I-state neighbors through the d'-simplex $[n_i,n_{j_0},n_{j_1}\cdots n_{j_{d'-1}}]$ with the enhanced infection probability $\nu_{d'}'\beta$ [corresponding to the process $\mathrm{Simp}(S,d'I)\xrightarrow{\nu_{d'}\beta}\mathrm{Simp}((d'+1)I)$]. For the spontaneous recovery process, it is operated by the node-independent recovery probability μ (i.e., $I\xrightarrow{\mu}R$). A recovered individual may lose immunity and then returns to the susceptible state by the node-independent probability of losing immunity γ (i.e., $R\xrightarrow{\gamma}S$). Note that when the order of a simplicial complex equals one (i.e., $d=1$), the susceptible nodes can only get an infection from their infected neighbors through the links, which means that the simplicial SIRS model reduces to the network-based SIRS model. The proposed simplicial SIRS model expands the SIS model[29] and provides an alternative perspective to understand the spreading process of complex systems by combining a nonlinear incidence rate with higher-order structures.

According to the definition of simplices, the collective interactions of a higher-order simplex include all the interactions of its sub-simplices. Taking 3-simplices as an example, they include not only the actions of the full triangles (i.e., 2-faces) on nodes but also the actions of links (i.e., 1-face) on nodes as well as the actions of nodes (i.e., 0-faces) on nodes. If we consider the contribution of all the high-dimension simplices, the computational complexity will be huge. Furthermore, according to system (1), only when all the other nodes in the simplex are infected, can the S-state node be infected by the enhanced probability. Thus, for a high-dimensional simplex of dimension d, the probability of d nodes being infected at the same time is tiny. Hence, taking all the factors into account, we just focus on the simplices of the dimension up to $d=2$ to explore the simplicial SIRS epidemic dynamics.

In order to better understand the simplicial SIRS model of $d=2$, we present an example, as shown in Fig. 1. Figures 1(a) and 1(b) present that the susceptible node n_i contacts with others through links (1-face) and can get an infection with probability β when it contacts an infected node. In Figs. 1(c) and 1(d), node n_i belongs to 2-simplices. For (c), due to the fact that other two nodes are infected, node n_i can get the infection from two pairwise interactions (corresponding to two 1-face) with probability β and

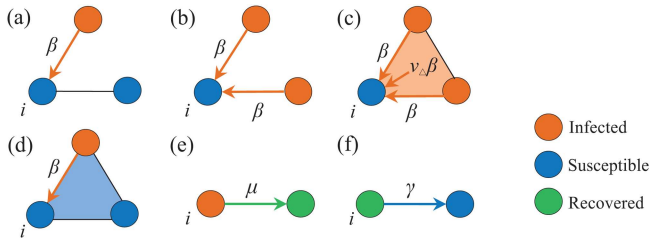

FIG. 1. The illustration for the simplicial SIRS model of order $d=2$. The infected, susceptible, and recovered nodes are colored in orange, blue, and green, respectively. (a) and (b) denote that the susceptible node n_i can only become infected from one or more infected neighbors through links (1-simplex). (c) and (d) represent the propagation behavior in 2-simplices. For (c), node n_i can get the infection through two links (1-face) and a triangle (2-faces), while for (c) node n_i can only get the infection through a link (1-face). (e) and (f) denote the spontaneous processes of recovery and losing immunity, respectively.

TABLE I. Statistics of real-world simplicial complexes.

Dataset	N	$\langle k \rangle$	$\langle k_\Delta \rangle$	ν_c
Karate	34	4.5882	3.9706	2.3111
Co-author	379	4.8232	7.2902	1.3232
Football	115	10.6609	21.1304	1.0091
Les Miserables	77	6.5974	18.1948	0.7252

from a collective interaction (corresponding to one 2-faces) with the enhanced probability $\nu_\Delta \beta$. But for (d), node n_i can become infected only through a pairwise interaction as there is only one infected node in this simplex. Figures 1(e) and 1(f) present that the infected and recovered nodes turn to the recovered and susceptible states with probabilities, μ and γ, respectively, corresponding to the processes of recovery and losing immunity.

III. RESULTS

In order to investigate the phenomenology of the proposed simplicial SIRS model with a nonlinear incidence rate, we first investigate the evolution over real-world simplicial complexes. The four publicly available networks are projected to their corresponding up to two-dimensional simplicial complexes, i.e., Karate club network,[60] Co-authorship network,[53] Football network,[61] and Les Miserables network.[62] Their connectivity properties are shown in Table I, where N, $\langle k \rangle$, and $\langle k_\Delta \rangle$ denote the number of nodes, the average degree, and the average number of 2-simplices, respectively, and ν_c is the critical point of ν_Δ, which is described in Eq. (9).

We simulate the simplicial SIRS dynamics over the four real-world simplicial complexes. In particular, two initial infectious densities $p^I(t=0)$ (i.e., 0.01 and 0.1) are adopted to iteratively obtain the stationary states, respectively. Figure 2 shows the spreading prevalence in the stationary state. The average infectious density $p^I_* = \frac{1}{N}\sum_{i=1}^{N} p_i^I(t \to \infty)$ in the stationary state is plotted as a function of the infectivity parameter β for $\nu_\Delta = 0.8\nu_c$ and $\nu_\Delta = 2.5\nu_c$. As a contrast, we also show the results for the case of $\nu_\Delta = 0$, which is equivalent to the standard SIRS model with no higher-order nonlinear reinforcement mechanism. Namely, there are two initial values for each ν_Δ. Therefore, actually each subgraph in Fig. 2 has six curves, where the relevant curves coincide when $\nu_\Delta = 0$ and $\nu_\Delta = 0.8\nu_c$. For $\nu_\Delta = 2.5\nu_c$, the leftmost curve corresponds to $p^I(t=0) = 0.1$ and another for $p^I(t=0) = 0.01$.

It is obvious that two different characteristics emerge for the two given values of $\nu_\Delta \neq 0$. For the nonlinear enhancement factor $\nu_\Delta = 0.8\nu_c$, the infectious density p^I_* evolutes with the infectivity parameter β in a similar way to that of $\nu_\Delta = 0$, with a continuous transition. But for $\nu_\Delta = 2.5\nu_c$, two discontinuous transitions occur when β crosses the two critical points [i.e., the epidemic thresholds, $\beta_c = \frac{\mu}{\langle k \rangle}$ and $\beta_0 = \frac{4\nu_\Delta \mu\gamma(\gamma+\mu)\langle k_\Delta \rangle}{(\nu_\Delta \gamma \langle k_\Delta \rangle + (\gamma+\mu)\langle k \rangle)^2}$, to be described in Eqs. (4) and (10) in detail], and we observe a bistable state that the healthy state $p^I_* = 0$ and the endemic state $p^I_* > 0$ can coexist. The bistable state phenomenon depends on the initial infectious density $p^I(t=0)$, that is, system (1) tends to the healthy state if $p^I(t=0) = 0.01$, while it tends to the endemic state if $p^I(t=0) = 0.1$.

Recalling that there exists a tipping point for minorities to change social convention,[63] we find that the initial values can affect the long-term state of the system for the simplicial SIRS model. When $p^I(t=0) = 0.01$, the threshold for epidemic outbreaks does not change for both $\nu_\Delta = 0.8\nu_c$ and $\nu_\Delta = 2.5\nu_c$, which is the same as that of the standard network case, β_c. But when $p^I(t=0) = 0.1$, a radical difference occurs that the spreading threshold varies for $\nu_\Delta = 2.5\nu_c$, i.e., from the standard threshold β_c to a smaller threshold β_0, as shown in the orange curves. The bistable state can occur when β is in the interval of $[\beta_0, \beta_c]$. We also find the bistable phenomenon that has been observed in a simplicial SIS model.[29]

Next, Fig. 3 shows the spreading prevalence of the simplicial SIRS model on the simplicial complexes constructed from two synthetic networks, i.e., an Erdös-Rényi (ER) random network[64] and a Watts-Strogatz (WS) small-world network.[65] The number of nodes and average degree of the two networks are set to $N = 200$ and $\langle k \rangle = 6$, respectively. The average number of 2-simplices is $\langle k_\Delta \rangle = 2.025$ for the simplicial complex from the ER network, and $\langle k_\Delta \rangle = 6.645$ for the WS network case. Similarly, we perform the numerical simulation on the two simplicial complexes by using the same initial values [i.e., $p^I(t=0) = 0.01$ and $p^I(t=0) = 0.1$]. It is clear that the overall evolution trend of Fig. 3 is the same as Fig. 2. Namely, the phenomena (i.e., the discontinuous transitions and bistable states) that appear in the real-world simplicial complexes also occur in the synthetic simplicial complexes.

The periodicity of epidemic outbreaks is an important topic in the field of disease transmission.[66–68] However, the standard SIRS model with bilinear incidence rates does not have periodic orbits,[69] and a few works consider higher-order interactions of a complex system to investigate the existence of periodic outbreak. For the proposed simplicial model that couples the higher-order structure with nonlinear incidence rates, we notice that the periodic phenomenon of epidemic outbreaks can occur under certain conditions. To explore this phenomenon in detail, we select a real network (i.e., the Les Miserables network) and a synthetic network [i.e., the same WS small-world network used in Fig. 3(b)] as examples. Simulation results show the periodic solutions and the stable limit cycles, as shown in Fig. 4. Compared with the simplicial SIS model, the proposed SIRS model is able to capture the periodicity of epidemic outbreaks, where the compartment "R" plays a major role. According to the simulation results above, both the real-world and synthetic cases yield similar conclusive results, thereby calling for further analysis in theory.

IV. DYNAMICAL ANALYSIS OF THE SIMPLICIAL SIRS MODEL

A. Mean-field approach

In order to further study the discontinuous transitions and the periodic phenomena of epidemic outbreaks, we simplify system (1) by introducing the mean-field (MF) approach under a homogeneous mixing assumption.[29] Hence, the MF description for the simplicial

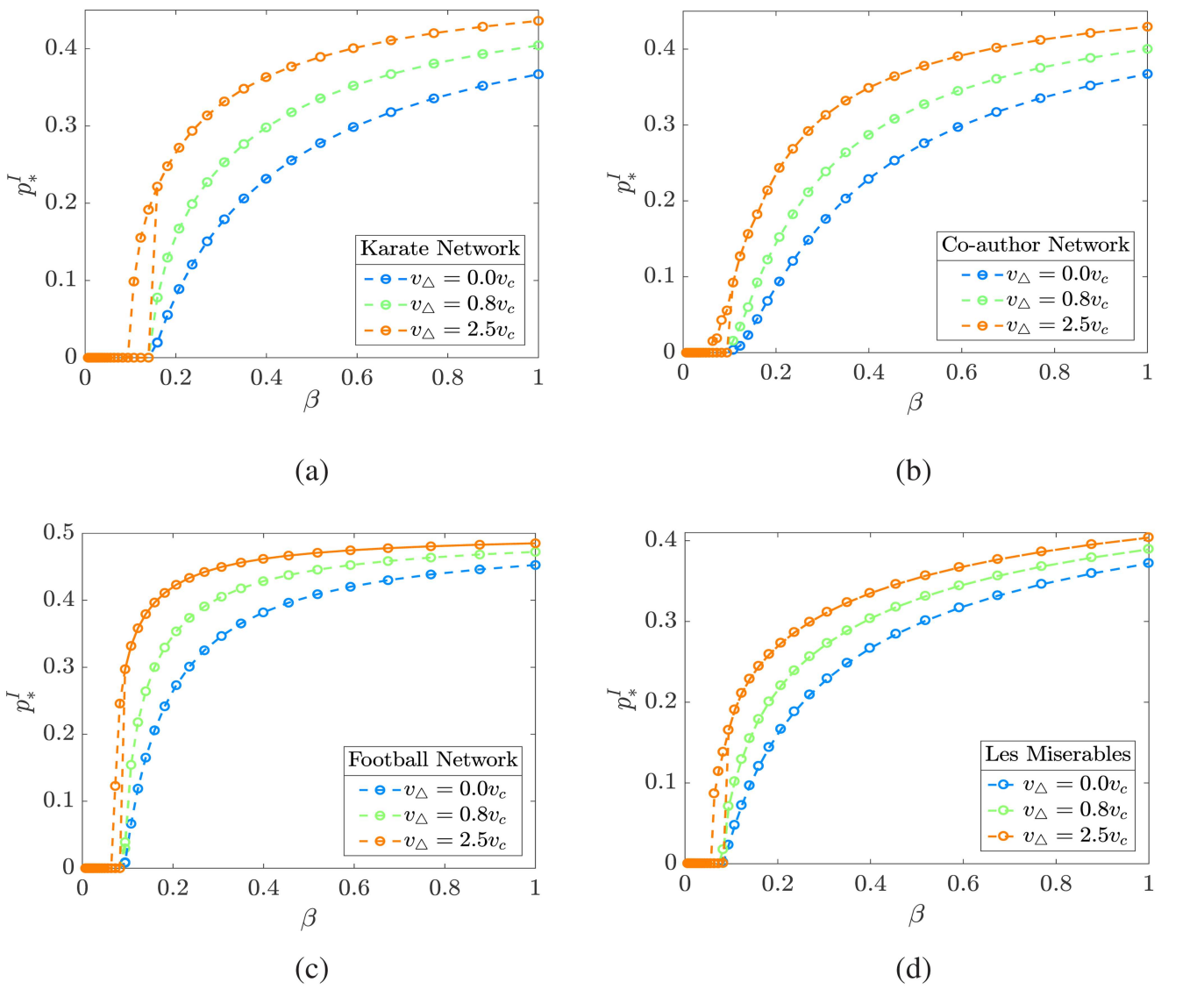

FIG. 2. The stationary spreading prevalence p_*^I of the simplicial SIRS model as a function of the infectivity parameter β for different nonlinear reinforcement $v_\triangle$ based on four simplicial complexes, which are constructed from four real-world networks: (a) Karate, (b) Co-author, (c) Football, and (d) Les Miserables. Here, $\gamma = \mu = 1$.

SIRS model of order $d = 2$ is written as

$$\begin{aligned}
\frac{dp^S(t)}{dt} &= -\beta p^S(t)\langle k\rangle p^I(t) - v_\triangle \beta p^S(t)\langle k_\triangle\rangle (p^I(t))^2 + \gamma p^R(t),\\
\frac{dp^I(t)}{dt} &= \beta p^S(t)\langle k\rangle p^I(t) + v_\triangle \beta p^S(t)\langle k_\triangle\rangle (p^I(t))^2 - \mu p^I(t),\\
\frac{dp^R(t)}{dt} &= \mu p^I(t) - \gamma p^R(t).
\end{aligned} \tag{2}$$

The limit set of system (2) is on the plane $p^S(t) + p^I(t) + p^R(t) = 1$ on which system (2) can be reduced to a two-dimensional system,

$$\begin{aligned}
\frac{dp^I(t)}{dt} &= \beta(1 - p^I(t) - p^R(t))\langle k\rangle p^I(t)\\
&\quad + v_\triangle \beta(1 - p^I(t) - p^R(t))\langle k_\triangle\rangle (p^I(t))^2 - \mu p^I(t),\\
\frac{dp^R(t)}{dt} &= \mu p^I(t) - \gamma p^R(t).
\end{aligned} \tag{3}$$

It is easy to obtain that $\Gamma = \{(p^I, p^R) | 0 \leqslant p^I \leqslant 1, 0 \leqslant p^R \leqslant 1\}$ is a positively invariant and bounded region for system (3).

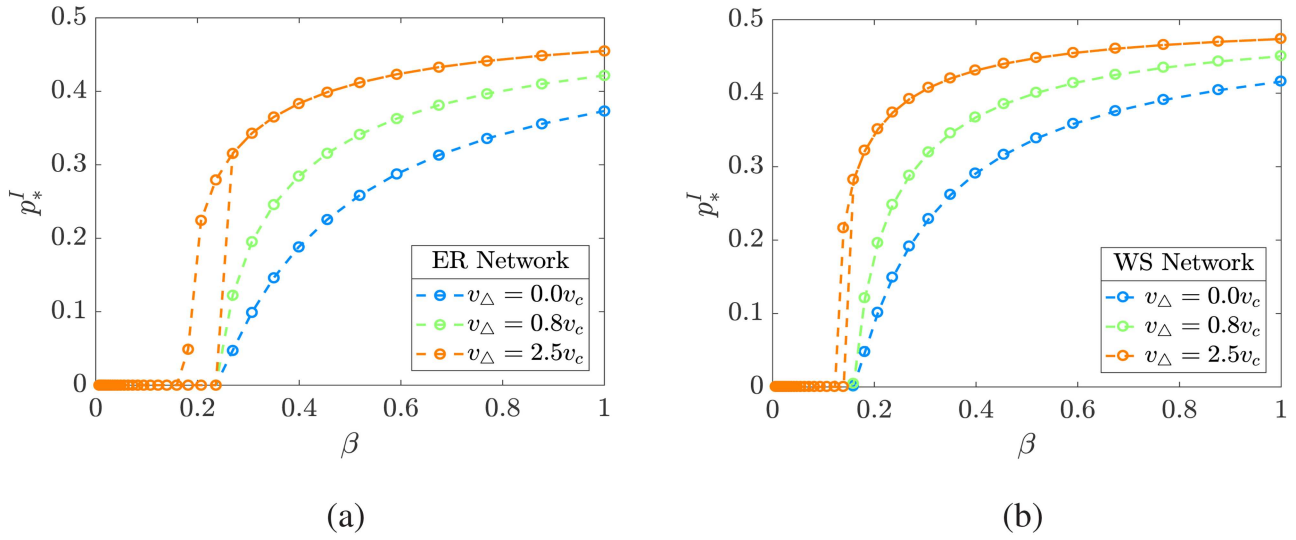

FIG. 3. The stationary spreading prevalence p_*^I of the simplicial SIRS model as a function of the infectivity parameter β for different nonlinear reinforcement v_Δ based on two simplicial complexes, which are constructed from two synthetic networks: (a) ER random network and (b) WS small-world network. Here, $\gamma = \mu = 1$.

First, we focus on the existence of equilibria of system (3). It is obvious that the infection-free equilibrium (IFE) of system (3) is $E_0 = (0, 0)$. Hence, by applying the next generation matrix method,[11] we get the threshold for epidemic outbreaks of system (3), which reads

$$\beta_c = \frac{\mu}{\langle k \rangle}. \tag{4}$$

The epidemic threshold β_c refers to the infectivity parameter required for epidemic outbreaks of the system under the small initial infectious condition. In such a case, the system tends to the healthy state when $\beta < \beta_c$.

An infection equilibrium $E_* = (p_*^I, p_*^R)$ is derived by solving

$$\begin{cases} 0 = \beta(1 - p_*^I(t) - p_*^R(t))\langle k \rangle p_*^I(t) + v_\Delta \beta(1 - p_*^I(t) \\ \quad -p_*^R(t))\langle k_\Delta \rangle (p_*^I(t))^2 - \mu p_*^I(t), \\ 0 = \mu p_*^I(t) - \gamma p_*^R(t). \end{cases}$$

It means $p_*^R = \frac{\mu}{\gamma} p_*^I$, and let

$$f(p_*^I) = A\left(p_*^I\right)^2 + B p_*^I + C, \tag{5}$$

where

$$\begin{aligned} A &= v_\Delta \beta \left\langle k_\Delta \right\rangle (\gamma + \mu) > 0, \\ B &= \beta \left[\mu \langle k \rangle - \gamma \left(v_\Delta \left\langle k_\Delta \right\rangle - \langle k \rangle\right)\right], \\ C &= \gamma(\mu - \beta \langle k \rangle), \end{aligned}$$

we thus can get p_*^I by solving $f(p_*^I) = 0$.

By denoting $\Delta = B^2 - 4AC$, two different roots of Eq. (5) are obtained if $\Delta > 0$,

$$p_{*1}^I = \frac{-B - \sqrt{\Delta}}{2A} \quad \text{and} \quad p_{*2}^I = \frac{-B + \sqrt{\Delta}}{2A}. \tag{6}$$

If $\Delta = 0$, p_{*1}^I coincides with p_{*2}^I.

To ensure the existence of an infection equilibrium in Γ, we require $p_*^R \in (0, 1]$, which means $0 < p_*^I \leq \min\{1, \frac{\gamma}{\mu}\}$. So, we need to investigate the positive roots of Eq. (5) in the interval $(0, \min\{1, \frac{\gamma}{\mu}\}]$. It is clear that

$$\begin{cases} f(0) = C = \gamma(\mu - \beta\langle k \rangle) = \gamma \langle k \rangle (\beta_c - \beta), \\ f(1) = A + B + C = \mu(\beta v_\Delta \left\langle k_\Delta \right\rangle + \beta \langle k \rangle + \gamma) > 0, \\ f\left(\frac{\gamma}{\mu}\right) = \frac{\beta \gamma^3 v_\Delta \left\langle k_\Delta \right\rangle}{\mu^2} + \frac{\beta \gamma^2 \langle k \rangle}{\mu} + \mu\gamma > 0. \end{cases} \tag{7}$$

Hence, if $\beta > \beta_c$, that is, $f(0) < 0$, $f(p_*^I) = 0$ has one positive root $p_{*2}^I \in (0, \min\{1, \frac{\gamma}{\mu}\}]$. As for $\beta < \beta_c$, which means $f(0) > 0$, $f(p_*^I) = 0$ admits two positive roots (denoted by p_{*1}^I and p_{*2}^I) in the interval $(0, \min\{1, \frac{\gamma}{\mu}\}]$ when $0 < -\frac{B}{2A} < \min\{1, \frac{\gamma}{\mu}\}$ and $\Delta > 0$. Similarly, if $\beta < \beta_c$, $0 < -\frac{B}{2A} < \min\{1, \frac{\gamma}{\mu}\}$ and $\Delta = 0$, then $f(p_*^I) = 0$ exists a unique positive root p_{**}^I $(= p_{*1}^I = p_{*2}^I)$ in $(0, \min\{1, \frac{\gamma}{\mu}\}]$.

Let $\Delta = 0$, i.e.,

$$\beta\left(\left(v_\Delta \gamma \left\langle k_\Delta \right\rangle + (\gamma + \mu)\langle k \rangle\right)^2 \beta - 4 v_\Delta \mu \gamma (\gamma + \mu) \left\langle k_\Delta \right\rangle\right) = 0,$$

we can get the expression of the enchantment factor, i.e.,

$$v_\Delta = \frac{\left(2\mu - \beta \left\langle k \right\rangle + 2\sqrt{\mu\left(\mu - \beta \left\langle k \right\rangle\right)}\right)(\gamma + \mu)}{\gamma \left\langle k_\Delta \right\rangle \beta}. \tag{8}$$

By replacing β in Eq. (8) with β_c in Eq. (4), we obtain the critical value of the enhancement factor

$$v_c = \frac{(\gamma + \mu)\langle k \rangle}{\gamma \left\langle k_\Delta \right\rangle}. \tag{9}$$

For $v_\Delta > v_c$, Eq. (5) may have two positive roots when $\beta < \beta_c$, but for $v_\Delta \leqslant v_c$, it does not have the positive roots when $\beta < \beta_c$.

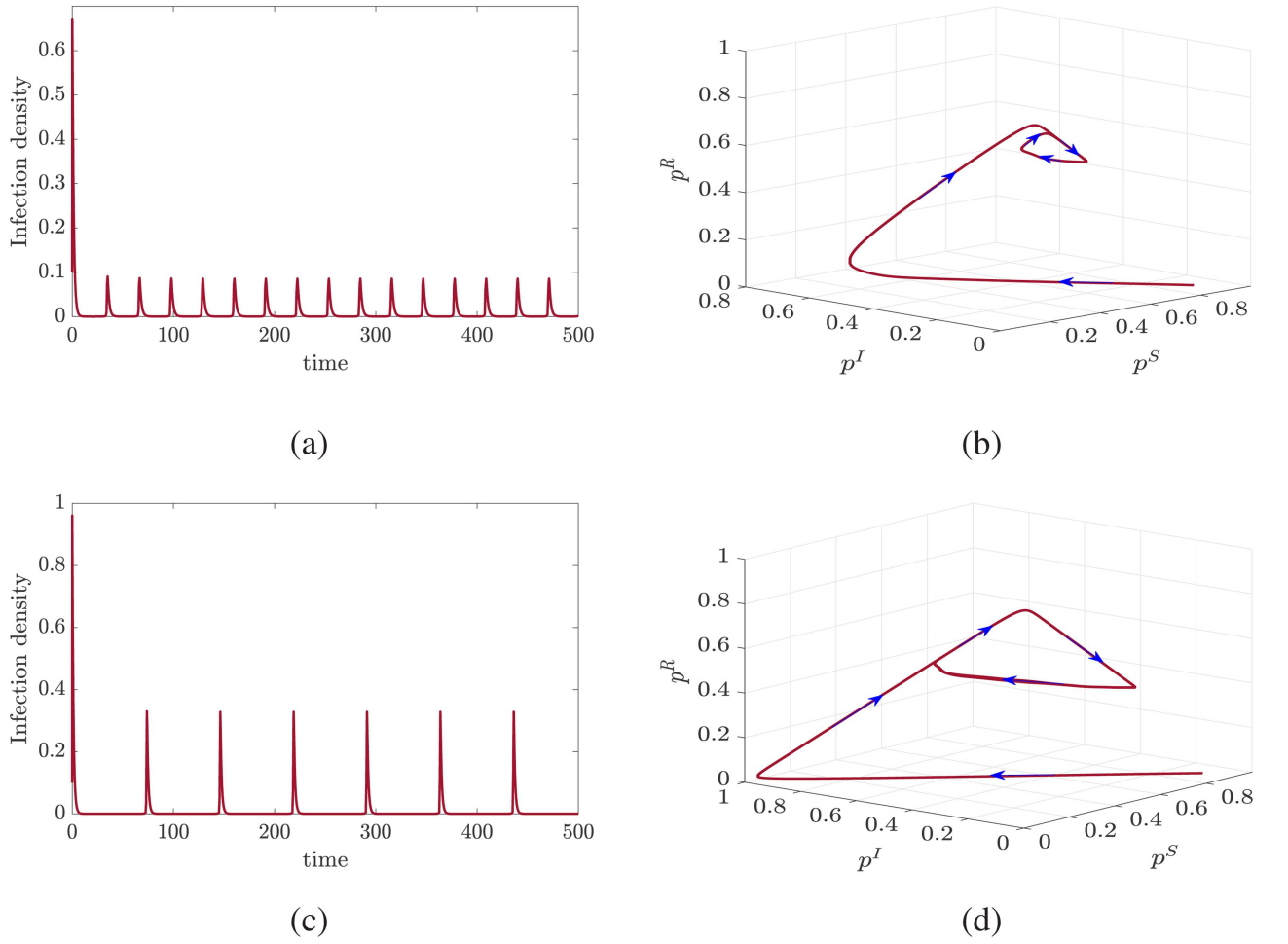

FIG. 4. The evolution of the spreading prevalence of the simplicial SIRS model on two networks: (a) Les Miserables and (c) WS small-world network, respectively. (b) and (d) the corresponding stable limit cycles of (a) and (c) represent the co-evolution of the three states. We also set $\nu_\Delta = 27.8$ for (a) and $\nu_\Delta = 88$ for (b), and $\beta = 0.5$, $\gamma = 0.01, \mu = 0.9$.

In a similar way, when $\nu_\Delta > \nu_c$, let $\Delta = 0$, we can derive the minimum infectivity parameter β_0 for $p^I_{*1} = p^I_{*2} > 0$,

$$\beta_0 = \frac{4\nu_\Delta \mu\gamma(\gamma+\mu)\langle k_\Delta\rangle}{\left(\nu_\Delta\gamma\langle k_\Delta\rangle + (\gamma+\mu)\langle k\rangle\right)^2}, \tag{10}$$

which is another epidemic threshold for the simplicial system. From the expressions of β_c and β_0, it is easy to confirm $\beta_0 < \beta_c$ in the case of $\nu_\Delta > \nu_c$. Furthermore, we can obtain that $\Delta < 0$ when $0 < \beta < \beta_0$, $\Delta = 0$ when $\beta = \beta_0$, and $\Delta > 0$ when $\beta > \beta_0$. We then conclude that system (3) always admits an infection-free equilibrium $E_0 = (0, 0)$ and a unique endemic infection equilibrium $E_{*2} = (p^I_{*2}, p^R_{*2})$ when $\beta > \beta_c$. Moreover, for $\nu_\Delta > \nu_c$, system (3) admits two endemic infection equilibria $E_{*1} = (p^I_{*1}, p^R_{*1})$ and $E_{*2} = (p^I_{*2}, p^R_{*2})$ when $\beta_0 \leqslant \beta < \beta_c$, where $E_{*1} = E_{*2}$ when $\beta = \beta_0$.

We further obtain the bifurcation characteristics of system (3). For $\nu_\Delta \leqslant \nu_c$, the system tends to the endemic state when $\beta > \beta_c$ and tends to the healthy state when $\beta < \beta_c$, so system (3) admits a forward bifurcation as β crosses the threshold β_c. In contrast, for $\nu_\Delta > \nu_c$, the corresponding bifurcation is backward. Moreover, in the case of $\nu_\Delta > \nu_c$, the system tends to the healthy state E_0 for $\beta \leqslant \beta_0$ but tends to endemic state E_{*2} for $\beta > \beta_0$, thereby indicating that the transition is discontinuous when β crosses β_0. If the initial infection size is small, we note that the system tends to the healthy state E_0 for $\beta \leqslant \beta_c$ but tends to endemic state E_{*2} for $\beta > \beta_c$, which indicates that the transition is also discontinuous when β crosses β_c. It is conclusive that for the proposed model with a nonlinear incidence rate, there exists a bistable region where the bistability phenomenon appears. By combining the two discontinuous transitions, we can obtain that the bistable region is the interval of $[\beta_0, \beta_c]$,

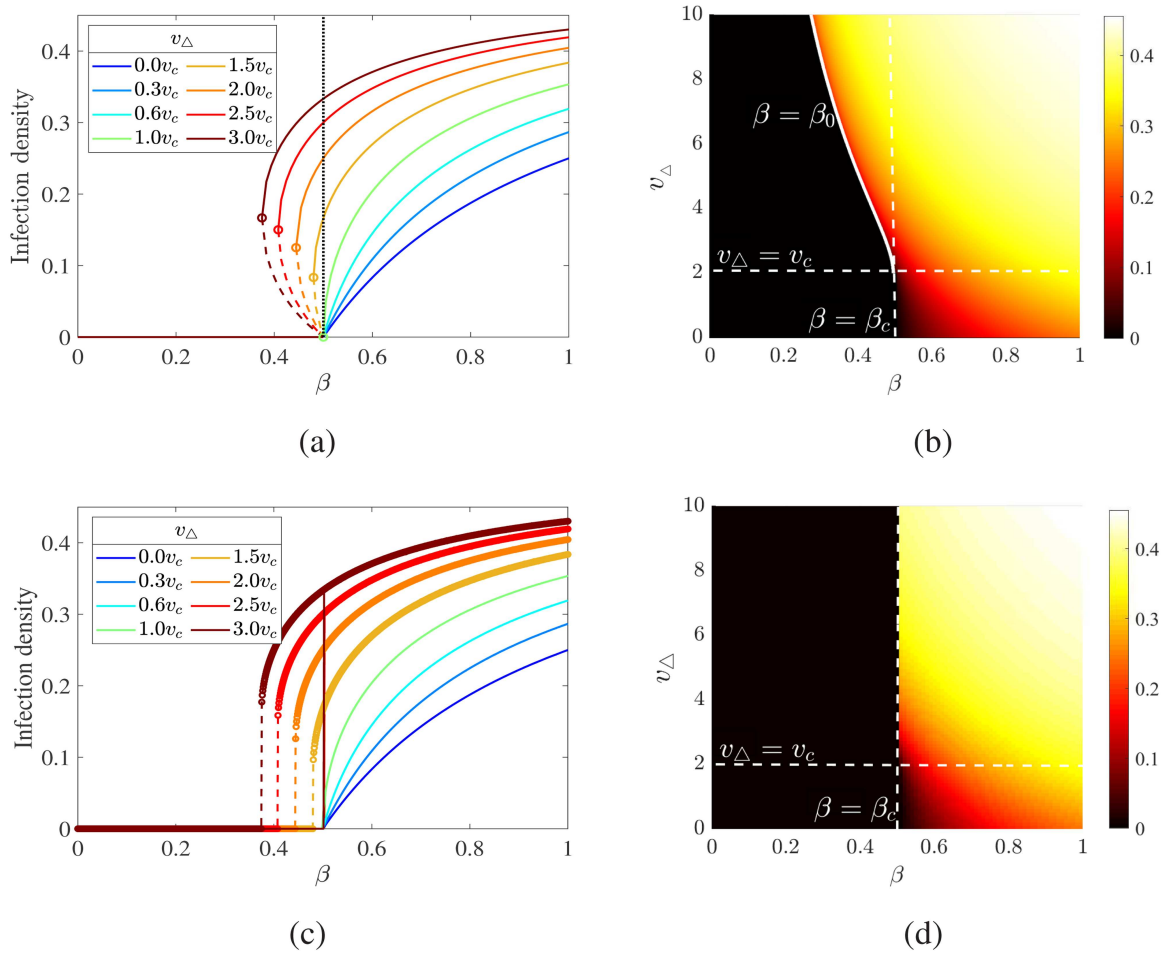

FIG. 5. Phase diagrams of the simplicial SIRS model. (a) The diagram of bifurcations of system (3), where the infectious density obtained by Eq. (6) is plotted as a function of β for different values of $v_\triangle$. The vertical line denotes the epidemic threshold $\beta_c = 0.5$. (b) The heatmap of the stationary state obtained by Eq. (6) as a function of β and $v_\triangle$. (c) and (d) are the results obtained by solving system (3), where the denotation is the same as (a) and (b), respectively. The parameters are $\langle k \rangle = \langle k_\triangle \rangle = 2$ and $\gamma = \mu = 1$.

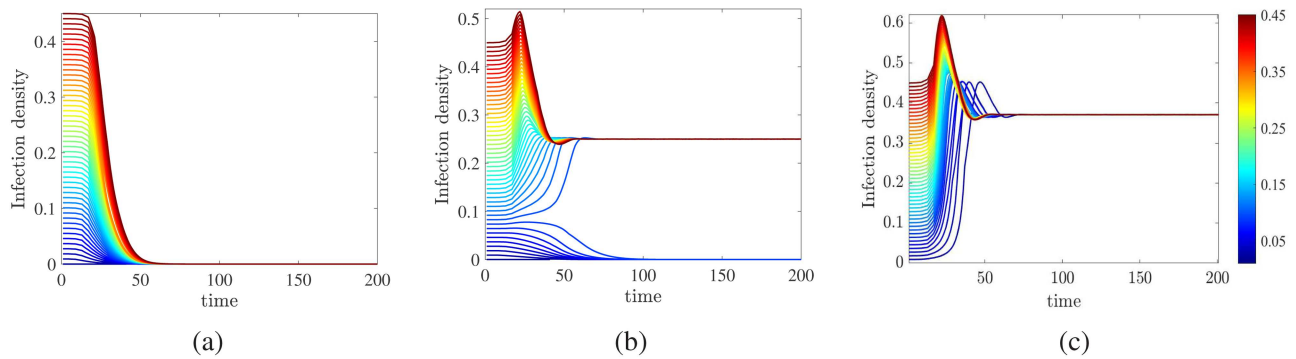

FIG. 6. The evolution of system (3) over time with different initial values for (a) $\beta = 0.2$, (b) $\beta = 0.4$, and (c) $\beta = 0.6$. The color bar denotes the initial density of the infected nodes $p^I(t = 0)$.

where the healthy and endemic states coexist. For another positive equilibrium E_{*1}, it is always unstable [to be described in Eq. (11)] so that the state of the system cannot asymptotically approach to it.

B. Stability analysis

Now, we study the stability of equilibria of system (3), which include E_0, E_{*1}, and E_{*2}. First, we investigate the stability of the infection-free equilibrium E_0. The Jacobian matrix of system (3) at E_0 is

$$J(E_0) = \begin{pmatrix} \beta\langle k\rangle - \mu & 0 \\ \mu & -\gamma \end{pmatrix}.$$

Then, we can derive

$$\det(J(E_0)) = -\gamma(\beta\langle k\rangle - \mu) = \gamma\langle k\rangle(\beta_c - \beta),$$

$$\mathrm{tr}(J(E_0)) = \beta\langle k\rangle - \mu - \gamma = \langle k\rangle(\beta - \beta_c) - \gamma.$$

Therefore, when $\beta < \beta_c$, we can conclude $\det(J(E_0)) > 0$ and $\mathrm{tr}(J(E_0)) < 0$, which imply that all the eigenvalues of the Jacobian matrix $J(E_0)$ have negative real parts under such conditions. According to the Routh–Hurwitz stability criterion, we can conclude the stability of E_0.

As for the stability of E_{*1}, we have the corresponding Jacobian matrix

$$J(E_{*1}) = \begin{pmatrix} -\beta\langle k\rangle p^I_{*1} + \nu_\Delta\beta\langle k_\Delta\rangle p^I_{*1}\left(1 - 2p^I_{*1} - \frac{\mu}{\gamma}p^I_{*1}\right) & -\beta\langle k\rangle p^I_{*1} - \nu_\Delta\beta\langle k_\Delta\rangle (p^I_{*1})^2 \\ \mu & -\gamma \end{pmatrix}. \tag{11}$$

By simple deduction, we get

$$\det(J(E_{*1})) = -Bp^I_{*1} - 2C = \frac{\sqrt{\Delta}}{2A}(\sqrt{\Delta} + B).$$

By the existence condition of E^I_{*1}, i.e., $\nu_\Delta > \nu_c$ and $\beta_0 < \beta < \beta_c$, we have $B < 0$ and $C > 0$ and then $0 < \sqrt{\Delta} < -B$, which means $\det(J(E_{*1})) < 0$. From that we derive the matrix $J(E_{*1})$ has a positive eigenvalue and then E_{*1} is unstable.

Similarly, we get the corresponding Jacobian matrix of system (3) at E_{*2} as follows:

$$J(E_{*2}) = \begin{pmatrix} -\beta\langle k\rangle p^I_{*2} + \nu_\Delta\beta\langle k_\Delta\rangle p^I_{*2}\left(1 - 2p^I_{*2} - \frac{\mu}{\gamma}p^I_{*2}\right) & -\beta\langle k\rangle p^I_{*2} - \nu_\Delta\beta\langle k_\Delta\rangle (p^I_{*2})^2 \\ \mu & -\gamma \end{pmatrix}$$

and then,

$$\det(J(E_{*2})) = \frac{\sqrt{\Delta}}{2A}(\sqrt{\Delta} - B),$$

$$\mathrm{tr}(J(E_{*2})) = -\beta\gamma\langle k_\Delta\rangle\nu_\Delta(p^I_{*2})^2 + \beta\langle k\rangle\mu p^I_{*2} - \gamma(\beta\langle k\rangle + \gamma - \mu).$$

Obviously, $\nu_\Delta > \nu_c$ and $\beta_0 < \beta < \beta_c$ imply $B < 0$ and then $\det(J(E_{*2})) > 0$. In addition, if $\beta > \beta_c$, then $C < 0$ and $\Delta > B^2$, which also means $\det(J(E_{*2})) > 0$. Hence, we can conclude $\det(J(E_{*2})) > 0$ always holds if E_{*2} exists. As for the sign of $\mathrm{tr}(J(E_{*2}))$, we observe that $\mathrm{tr}(J(E_{*2})) \geqslant 0$ may occur when the recovery probability μ is much larger than the losing immunity probability γ (for instance, the parameter values $\mu = 0.9$, $\gamma = 0.01$, $\langle k\rangle = 6$, $\langle k_\Delta\rangle = 6.65$, $\nu_\Delta = 88$, and $\beta = 0.5$), which means that $\mathrm{tr}(J(E_{*2})) < 0$ needs to be satisfied under some conditions. Define

$$\Delta' = (\beta\langle k\rangle\mu)^2 - 4\beta\gamma^2\langle k_\Delta\rangle\nu_\Delta(\beta\langle k\rangle + \gamma - \mu),$$

$$P^-_* = \frac{\beta\langle k\rangle\mu - \sqrt{\Delta'}}{2\beta\gamma\langle k_\Delta\rangle\nu_\Delta}, \quad P^+_* = \frac{\beta\langle k\rangle\mu + \sqrt{\Delta'}}{2\beta\gamma\langle k_\Delta\rangle\nu_\Delta}.$$

Then, we can derive three conditions of $\mathrm{tr}(J(E_{*2})) < 0$: (1) $\Delta' < 0$; (2) $\Delta' > 0$ and $p^I_{*2} < P^-_*$; and (3) $\Delta' > 0$ and $p^I_{*2} > P^+_*$. When one of the three conditions is satisfied, the equilibrium E_{*2} is stable. Otherwise, we get $\mathrm{tr}(J(E_{*2})) \geqslant 0$, then the equilibrium E_{*2} is unstable and system (3) can occur periodic oscillation. We, therefore, conclude the stability of E_0, E_{*1}, and E_{*2}: (1) the infection-free equilibrium E_0 is asymptotically stable if $\beta < \beta_c$ and is unstable if $\beta > \beta_c$; (2) the

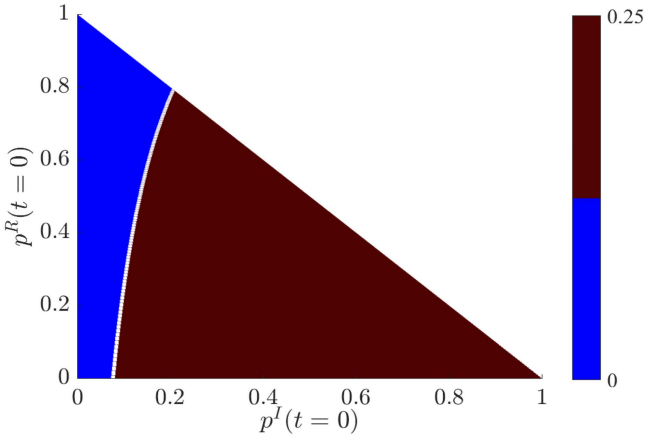

FIG. 7. The stationary infectious density p^I_* as a function of initial infection probability $p^I(t=0)$ and initial recovery probability $p^R(t=0)$, where the healthy and endemic states are marked in blue and purple, respectively. The parameter settings are the same as Fig. 6(b).

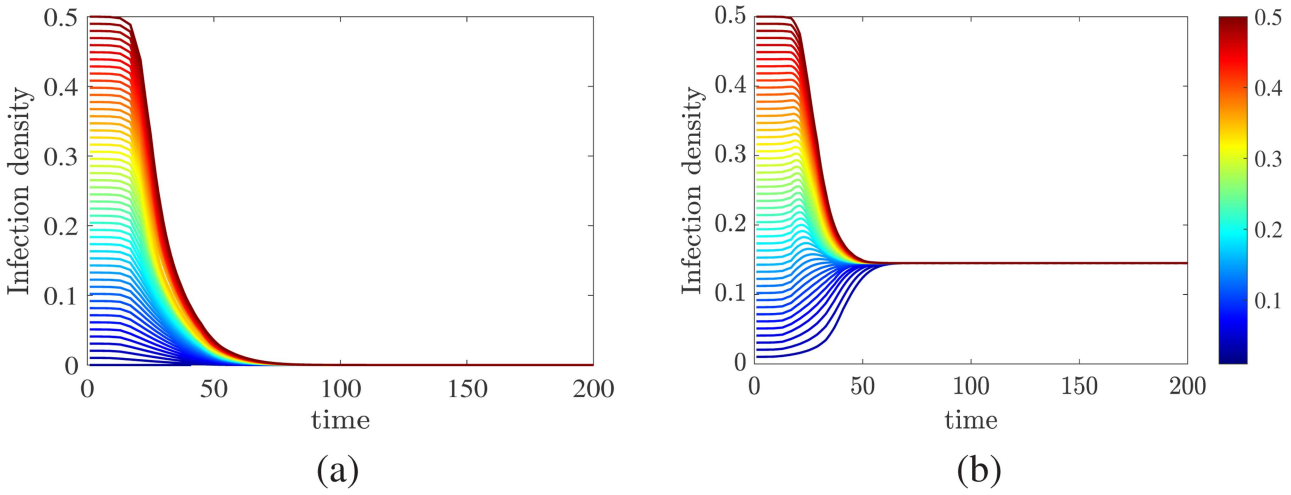

FIG. 8. The evolution of system (3) over time with different initial values. The colorbar denotes the initial density of infected nodes $p^I(t=0)$. The parameters are set to $\langle k\rangle = \langle k_\Delta\rangle = 2$, $\gamma = \mu = 1$, $\nu_\Delta = 0.6\nu_c$ for (a) $\beta = 0.4$ and (b) $\beta = 0.6$.

endemic infection equilibrium E_{*1} is always unstable; and (3) the endemic infection equilibrium E_{*2} is conditionally stable and can oscillate periodically under the certain conditions.

C. Numerical validation

Next, we perform simulations to verify the theoretical results, including the bistable states, the discontinuous transitions, and limit cycles. In Fig. 5(a), we observe a forward bifurcation when $\nu_\Delta \leqslant \nu_c$ and a backward bifurcation when $\nu_\Delta > \nu_c$. When system (3) admits a forward bifurcation, the non-negative initial values with a fixed β do not affect the final state of variables, and β_c is the threshold of epidemic eliminated. However, for the backward bifurcation, $\beta < \beta_c$ is not sufficient to eliminate an epidemic. In such a case, $\beta < \beta_0$ is a sufficient and necessary condition to eliminate an epidemic with various initial values. When $\beta_0 < \beta < \beta_c$, the phenomena of the bistable states emerge, and the initial values impact the stationary states of system (3). In other words, a critical initial infection density is required to reach the stationary endemic state, which is consistent with the finding that a tipping point of a committed minority exists to change social convention.[63]

The two-dimensional diagram of p^I_{*2} as a function of β and ν_Δ is shown in Fig. 5(b), which just exhibits the stationary results of systems (3) under a certain initial infection size. The lighter colors associate with the higher values of infection density, and the dashed vertical line associates with the epidemic threshold of the standard SIRS model. For $\nu_\Delta \leqslant \nu_c$ (below the dashed horizontal line), the transition as β crosses β_c appears to be continuous. In contrast,

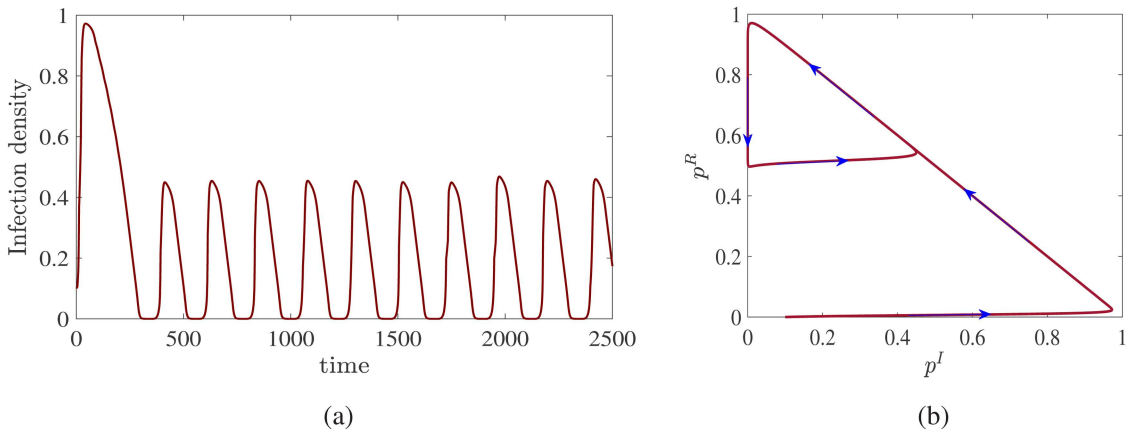

FIG. 9. (a) The evolution of system (3) over time with the initial value $p^I(t=0) = 0.1$. (b) The phase diagram between the infectious density $p^I(t)$ and the recovery density $p^R(t)$.

for $\nu_\Delta > \nu_c$, we observe a shift of the epidemic threshold (i.e., the changing β_0) and a discontinuous transition when β crosses β_0. We note that the critical curve β_0 marked in the white curve can also be derived by Eq. (10).

By numerically integrating system (3), we obtain Fig. 5(c) with the two initial infection densities $p^I(t=0) = 10^{-4}$ and $p^I(t=0) = 0.2$ for various ν_Δ, where the corresponding results are denoted by the solid and dashed lines, respectively. The results for $p^I(t=0) = 0.2$ with $\nu_\Delta > \nu_c$ are also marked with circles. It is obvious that the transition is continuous for the two initial infection densities when $\nu_\Delta \leqslant \nu_c$. Conversely, the discontinuous phenomena occur when $\nu_\Delta > \nu_c$. We notice that the critical points of the discontinuous transition are different for the two different initial infection densities: the standard threshold β_c for $p^I(t=0) = 10^{-4}$, showed by the solid lines, and β_0 for $p^I(t=0) = 0.2$, showed by the dashed circle lines. Under certain conditions, epidemics can break out at a lower threshold β_0 rather than the normal threshold β_c, which may explain why epidemics break out so quickly.[70] We note that the standard threshold β_c [computed by Eq. (4)] is a fixed value independent of ν_Δ while β_0 [computed by Eq. (10)] is a variable negatively related to ν_Δ. In the interval of $[\beta_0, \beta_c]$, we can see the bistable phenomenon where the endemic equilibrium and infection-free equilibrium coexist. As a comparison with Figs. 5(b) and 5(d) shows the stationary states of system (3) at the tiny initial infection condition $p^I(t=0) = 10^{-4}$. It is clear that β_c is the epidemic threshold and the discontinuous transitions occur along the β_c line for $\nu_\Delta > \nu_c$, which is consistent with the previous theoretical analysis.

In order to more concretely explore the bistable phenomena of system (3) , taking the parameters $\langle k\rangle = \langle k_\Delta\rangle = 2$, $\gamma = \mu = 1$ and $\nu_\Delta = 3\nu_c$ as an example, we implement the numerical simulations of system (3) over time for various values of β, as shown in Fig. 6. System (3) exhibits a backward bifurcation, and we obtain the two thresholds for the epidemic outbreak, i.e., $\beta_0 = 0.375$ and $\beta_c = 0.5$. For $\beta = 0.2 < \beta_0$, Fig. 6 shows that all the numerical solutions tend to an infection-free equilibrium for various initial values. When $\beta_0 < \beta = 0.4 < \beta_c$, Fig. 6(b) presents two stable equilibria (an infection-free equilibrium E_0 and an endemic infection equilibrium E_{*2}) so system (3) exhibits a bistable state where the initial values impact the dynamics of system (3). It indicates that there exists a critical initial infectious density that determines whether the long-term dynamics reaches the endemic state or the healthy one. As a result, if the initial infectious density exceeds a certain size, then the epidemic will spread instead of becoming extinct. When $\beta = 0.6 > \beta_c$, only an endemic infection equilibrium E_{*2} is stable and the numerical solutions approach to it, as shown in Fig. 6(c).

In the simplicial SIS model, the unstable equilibrium p^I_{1*} is the critical initial value to discriminate the long-term healthy state and the endemic state. But for the proposed SIRS model, p^I_{1*} is not the critical initial value anymore. In order to investigate the influence of initial values on the simplicial system (3), we perform experiments to obtain the stationary infection density p^I_* as a function of $p^I(t=0)$ and $p^R(t=0)$. As shown in Fig. 7, it is clear that the critical white curve separates the healthy and endemic states. Namely, the system tends to the healthy state when the initial values are on the left side of the white curve and tends to the endemic state when the initial values are on the right side of the white curve.

We then investigate the evolution of equilibrium of system (3) for the scenario of $\nu_\Delta \leqslant \nu_c$. In such case, system (3) exhibits a forward bifurcation which means that the infection-free equilibrium E_0 is stable when $\beta < \beta_c$ and the endemic infection equilibrium E_{*2} is stable when $\beta > \beta_c$. Taking $\nu_\Delta = 0.6\nu_c$ as an example, we simulate the evolution of system (3) for $\beta = 0.4$ and $\beta = 0.6$, which are presented in Figs. 8(a) and 8(b), respectively.

All the above figures present that the existing equilibrium E_{*2} is stable. However, distinct from the simplicial SIS model, the endemic state E_{*2} of the simplicial system is not always stable in the SIRS case. In order to detect the periodic phenomena of epidemic outbreaks, we investigate the dynamics of system (3) when the stability conditions are not satisfied. We then fix the same parameters as Fig. 4(c), i.e.,

$$\langle k\rangle = 6,\ \langle k_\Delta\rangle = 6.645,\ \gamma = 0.01,\ \mu = 0.9,\ \nu_\Delta = 88,\ \beta = 0.5.$$

By numerical simulation, we obtain that E_{*2} is unstable and system (3) exhibits a periodic solution, as presented in Fig. 9. Actually such periodic epidemic outbreaks exist in real life, such as the spread of dengue.[71] Distinct from the network-based SIRS and simplicial SIS models, the proposed simplicial SIRS model can capture richer dynamical behaviors, thereby providing an alternative approach to model the actual epidemics.

V. CONCLUSIONS

In summary, the proposed simplicial SIRS epidemic model takes account of the higher-order topology of complex networks and a nonlinear incidence rate to study collective interactions, which is found to bring about richer dynamical phenomena. By performing extensive experiments, we examine the higher-order simplicial SIRS dynamics on simplicial complexes constructed from the real-world and synthetic networks. When the enhancement factor is larger than the critical value, the spreading transition becomes discontinuous when the infectivity parameter crosses the two epidemic thresholds. When the infectivity parameter is between the two thresholds, the healthy state and the endemic state can coexist, which is consistent with the emergent behavior in SIS models. More importantly, by introducing the more states in the epidemic models, like the recovery state (i.e., the R state), we observe the periodic phenomenon of epidemic outbreaks and the stable limit cycles in the simplicial SIRS model.

Moreover, we implement theoretical analysis toward the simplicial SIRS model based on the mean-field approximation. Two thresholds for epidemic outbreaks and the critical value of the enhancement factor are derived. For the enhancement factor larger than the critical value, the discontinuous transitions caused by higher-order interactions occur. In particular, the condition for the existence of limit cycles is derived. Furthermore, we present the stability of the equilibrium points, which is helpful to understand the stability characteristics of simplicial systems. The theoretical results confirm the findings obtained in simulations, which indicates that the simplicial framework is an effective and reliable framework for understanding complex spreading dynamics on higher-order systems.

ACKNOWLEDGMENTS

We are grateful to the referees for careful reading and valuable comments which lead to important improvements in our original manuscript. This work was supported by an Innovative Research Project of Shenzhen under Project No. KQJSCX20180328165509766 and the Natural Science Foundation of Guangdong, China under Grant No. 2020A1515010812.

DATA AVAILABILITY

The data that support the findings of this study are openly available at https://github.com/gephi/gephi/wiki/Datasets, Ref. 72.

REFERENCES

[1]R. Pastor-Satorras, C. Castellano, P. Van Mieghem, and A. Vespignani, "Epidemic processes in complex networks," Rev. Mod. Phys. **87**, 925–979 (2015).
[2]T. W. Valente, "Network models of the diffusion of innovations," Comput. Math. Organ. Theory **2**, 163–164 (1996).
[3]R. Cowan and N. Jonard, "Network structure and the diffusion of knowledge," J. Econ. Dyn. Control **28**, 1557–1575 (2004).
[4]I. Iacopini, S. Milojevic, and V. Latora, "Network dynamics of innovation processes," Phys. Rev. Lett. **120**, 048301 (2018).
[5]D. J. Watts and P. S. Dodds, "Influentials, networks, and public opinion formation," J. Consum. Res. **34**, 441–458 (2007).
[6]I. Z. Kiss, J. C. Miller, P. L. Simon *et al.*, *Mathematics of Epidemics on Networks*, (Springer, Cham, 2017), Vol. 598.
[7]S. Gómez, A. Arenas, J. Borge-Holthoefer, S. Meloni, and Y. Moreno, "Discrete-time Markov chain approach to contact-based disease spreading in complex networks," Europhys. Lett. **89**, 38009 (2010).
[8]M. Shrestha and C. Moore, "Message-passing approach for threshold models of behavior in networks," Phys. Rev. E **89**, 022805 (2014).
[9]C.-R. Cai, Z.-X. Wu, and J.-Y. Guan, "Effective degree Markov-chain approach for discrete-time epidemic processes on uncorrelated networks," Phys. Rev. E **90**, 052803 (2014).
[10]J. T. Matamalas, A. Arenas, and S. Gómez, "Effective approach to epidemic containment using link equations in complex networks," Sci. Adv. **4**, eaau4212 (2018).
[11]P. van den Driessche and J. Watmough, "Reproduction numbers and subthreshold endemic equilibria for compartmental models of disease transmission," Math. Biosci. **180**, 29–48 (2002).
[12]C. Castellano and R. Pastor-Satorras, "Thresholds for epidemic spreading in networks," Phys. Rev. Lett. **105**, 218701 (2010).
[13]C. Granell, S. Gomez, and A. Arenas, "Dynamical interplay between awareness and epidemic spreading in multiplex networks," Phys. Rev. Lett. **111**, 128701 (2013).
[14]G. F. de Arruda, F. A. Rodrigues, and Y. Moreno, "Fundamentals of spreading processes in single and multilayer complex networks," Phys. Rep. **756**, 1–59 (2018).
[15]A. V. Goltsev, S. N. Dorogovtsev, J. G. Oliveira, and J. F. Mendes, "Localization and spreading of diseases in complex networks," Phys. Rev. Lett. **109**, 128702 (2012).
[16]G. F. de Arruda, E. Cozzo, T. P. Peixoto, F. A. Rodrigues, and Y. Moreno, "Disease localization in multilayer networks," Phys. Rev. X **7**, 011014 (2017).
[17]H. F. Zhang, J. R. Xie, M. Tang, and Y. C. Lai, "Suppression of epidemic spreading in complex networks by local information based behavioral responses," Chaos **24**, 043106 (2014).
[18]S. Funk, E. Gilad, C. Watkins, and V. A. A. Jansen, "The spread of awareness and its impact on epidemic outbreaks," Proc. Natl. Acad. Sci. U.S.A. **106**, 6872–6877 (2009).
[19]M. Kitsak, L. K. Gallos, S. Havlin, F. Liljeros, L. Muchnik, H. E. Stanley, and H. A. Makse, "Identification of influential spreaders in complex networks," Nat. Phys. **6**, 888–893 (2010).
[20]Y. Hu, S. Ji, Y. Jin, L. Feng, H. E. Stanley, and S. Havlin, "Local structure can identify and quantify influential global spreaders in large scale social networks," Proc. Natl. Acad. Sci. U.S.A. **115**, 7468–7472 (2018).
[21]L. Y. Lu, D. B. Chen, X. L. Ren, Q. M. Zhang, Y. C. Zhang, and T. Zhou, "Vital nodes identification in complex networks," Phys. Rep. **650**, 1–63 (2016).
[22]J. L. Burton, "Health and safety at necropsy," J. Clin. Pathol. **56**, 254–260 (2003).
[23]J. W. Tang, P. Wilson, N. Shetty, and C. J. Noakes, "Aerosol-transmitted infections—A new consideration for public health and infection control teams," Curr. Treat. Options Infect. Dis. **7**, 176–201 (2015).
[24]B. J. Rijnders, J. J. Cornelissen, L. Slobbe, M. J. Becker *et al.*, "Aerosolized liposomal amphotericin B for the prevention of invasive pulmonary aspergillosis during prolonged neutropenia: A randomized, placebo-controlled trial," Clin. Infect. Dis. **46**, 1401–1408 (2008).
[25]R. Lambiotte, M. Rosvall, and I. Scholtes, "From networks to optimal higher-order models of complex systems," Nat. Phys. **15**, 313–320 (2019).
[26]F. Battiston, G. Cencetti, I. Iacopini, V. Latora, M. Lucas, A. Patania, J.-G. Young, and G. Petri, "Networks beyond pairwise interactions: Structure and dynamics," Phys. Rep. **874**, 1–92 (2020).
[27]A. Barrat, G. F. de Arruda, I. Iacopini, and Y. Moreno, "Social contagion on higher-order structures," arXiv:2103.03709 [physics.soc-ph] (2021).
[28]A. Bodó, G. Y. Katona, and P. L. Simon, "SIS epidemic propagation on hypergraphs," Bull. Math. Biol. **78**, 713–735 (2016).
[29]I. Iacopini, G. Petri, A. Barrat, and V. Latora, "Simplicial models of social contagion," Nat. Commun. **10**, 2485 (2019).
[30]G. F. de Arruda, G. Petri, and Y. Moreno, "Social contagion models on hypergraphs," Phys. Rev. Res. **2**, 023032 (2020).
[31]G. F. de Arruda, M. Tizzani, and Y. Moreno, "Phase transitions and stability of dynamical processes on hypergraphs," Commun. Phys. **4**, 24 (2021).
[32]T. Carletti, F. Battiston, G. Cencetti, and D. Fanelli, "Random walks on hypergraphs," Phys. Rev. E **101**, 022308 (2020).
[33]D. J. Higham and H.-L. de Kergorlay, "Epidemics on hypergraphs: Spectral thresholds for extinction," arXiv:2103.07319 [cs.SI] (2021).
[34]J. J. Torres and G. Bianconi, "Simplicial complexes: Higher-order spectral dimension and dynamics," J. Phys. Complexity **1**, 015002 (2020).
[35]D. Wang, Y. Zhao, H. Leng, and M. Small, "A social communication model based on simplicial complexes," Phys. Lett. A **384**, 126895 (2020).
[36]G. Burgio, A. Arenas, S. Gómez, and J. T. Matamalas, "Network clique cover approximation to analyze complex contagions through group interactions," arXiv:2101.03618 [physics.soc-ph] (2021).
[37]F. Ball and P. Donnelly, "Strong approximations for epidemic models," Stoch. Process. Their Appl. **55**, 1–21 (1995).
[38]A. Margheri and C. Rebelo, "Some examples of persistence in epidemiological models," J. Math. Biol. **46**, 564 (2003).
[39]X. Y. Li and W. D. Wang, "A discrete epidemic model with stage structure," Chaos, Solitons Fractals **26**, 947–958 (2005).
[40]M. Alexander and S. Moghadas, "Periodicity in an epidemic model with a generalized non-linear incidence," Math. Biosci. **189**, 75–96 (2004).
[41]W. R. Derrick and P. van den Driessche, "A disease transmission model in a nonconstant population," J. Math. Biol. **31**, 495–512 (1993).
[42]V. Vuorinen, M. Aarnio, M. Alava, V. Alopaeus *et al.*, Modelling aerosol transport and virus exposure with numerical simulations in relation to SARS-CoV-2 transmission by inhalation indoors," Saf. Sci. **130**, 104866 (2020).
[43]P. Srikanth, S. Sudharsanam, and R. Steinberg, "Bio-aerosols in indoor environment: Composition, health effects and analysis," Indian J. Med. Microbiol. **26**, 302 (2008).
[44]V. Capasso and G. Serio, "A generalization of the Kermack-McKendrick deterministic epidemic model," Math. Biosci. **42**, 43–61 (1978).
[45]W.-M. Liu, S. A. Levin, and Y. Iwasa, "Influence of nonlinear incidence rates upon the behavior of SIRS epidemiological models," J. Math. Biol. **23**, 187–204 (1986).
[46]W.-M. Liu, H. W. Hethcote, and S. A. Levin, "Dynamical behavior of epidemiological models with nonlinear incidence rates," J. Math. Biol. **25**, 359–380 (1987).
[47]S. Ruan and W. Wang, "Dynamical behavior of an epidemic model with a nonlinear incidence rate," J. Differ. Equations **188**, 135–163 (2003).

[48]P. van den Driessche and J. Watmough, "A simple SIS epidemic model with a backward bifurcation," J. Math. Biol. **40**, 525–540 (2000).
[49]Y. Jin, W. Wang, and S. Xiao, "An SIRS model with a nonlinear incidence rate," Chaos, Solitons Fractals **34**, 1482–1497 (2007).
[50]Y. Muroya and T. Kuniya, "Global stability for a delayed multi-group SIRS epidemic model with cure rate and incomplete recovery rate," Int. J. Biomath. **08**, 1550048 (2015).
[51]V. Salnikov, D. Cassese, and R. Lambiotte, "Simplicial complexes and complex systems," Eur. J. Phys. **40**, 014001 (2019).
[52]O. T. Courtney and G. Bianconi, "Generalized network structures: The configuration model and the canonical ensemble of simplicial complexes," Phys. Rev. E **93**, 062311 (2016).
[53]M. E. Newman, "Finding community structure in networks using the eigenvectors of matrices," Phys. Rev. E **74**, 036104 (2006).
[54]D. Kozlov, *Combinatorial Algebraic Topology*, Algorithms and Computation in Mathematics (Springer-Verlag, Berlin, 2008).
[55]B. J. Stolz, H. A. Harrington, and M. A. Porter, "Persistent homology of time-dependent functional networks constructed from coupled time series," Chaos **27**, 047410 (2017).
[56]S. Maletic, Y. Zhao, and M. Rajkovic, "Persistent topological features of dynamical systems," Chaos **26**, 053105 (2016).
[57]A. Hatcher, *Algebraic Topology* (Cambridge University Press, Cambridge, 2002).
[58]L. V. Gambuzza, F. Di Patti, L. Gallo, S. Lepri, M. Romance, R. Criado, M. Frasca, V. Latora, and S. Boccaletti, "Stability of synchronization in simplicial complexes," Nat. Commun. **12**, 1255 (2021).
[59]Y. Wang, D. Chakrabarti, C. Wang, and C. Faloutsos, "Epidemic spreading in real networks: an eigenvalue viewpoint," in *22nd International Symposium on Reliable Distributed Systems*, (2003), pp. 25–34.
[60]W. W. Zachary, "An information flow model for conflict and fission in small groups," J. Anthropol. Res. **33**, 452–473 (1977).
[61]M. Girvan and M. E. Newman, "Community structure in social and biological networks," Proc. Natl. Acad. Sci. U.S.A. **99**, 7821–7826 (2002).
[62]D. E. Knuth, *The Stanford GraphBase: A Platform for Combinatorial Computing* (ACM Press, New York, 1993).
[63]D. Centola, J. Becker, D. Brackbill, and A. Baronchelli, "Experimental evidence for tipping points in social convention," Science **360**, 1116–1119 (2018).
[64]P. Erdős and A. Rényi, "On the evolution of random graphs," Publ. Math. **5**, 17–60 (1960).
[65]D. J. Watts and S. H. Strogatz, "Collective dynamics of 'small-world' networks," Nature **393**, 440–442 (1998).
[66]H. W. Hethcote and S. A. Levin, "Periodicity in epidemiological models," in *Applied Mathematical Ecology*, edited by S. A. Levin, T. G. Hallam, and L. J. Gross (Springer, Berlin, 1989), pp. 193–211.
[67]A. Uziel and L. Stone, "Determinants of periodicity in seasonally driven epidemics," J. Theor. Biol. **305**, 88–95 (2012).
[68]M. Hooshyar, C. E. Wagner, R. E. Baker, C. J. E. Metcalf, B. T. Grenfell, and A. Porporato, "Cyclic epidemics and extreme outbreaks induced by hydro-climatic variability and memory," J. R. Soc. Interface **17**, 20200521 (2020).
[69]H. Jardón-Kojakhmetov, C. Kuehn, A. Pugliese, and M. Sensi, "A geometric analysis of the SIR, SIRS and SIRWS epidemiological models," Nonlinear Anal.: Real World Appl. **58**, 103220 (2021).
[70]M. Tizzoni, P. Bajardi, A. Decuyper, G. Kon Kam King, C. M. Schneider, V. Blondel, Z. Smoreda, M. C. González, and V. Colizza, "On the use of human mobility proxies for modeling epidemics," PLoS Comput. Biol. **10**, 1–15 (2014).
[71]B. P. Gupta, R. Tuladhar, R. Kurmi, and K. D. Manandhar, "Dengue periodic outbreaks and epidemiological trends in Nepal," Ann. Clin. Microbiol. Antimicrob. **17**, 6 (2018).
[72]Richirikken, Datasets https://github.com/gephi/gephi/wiki/Datasets.